Evidence that Mechanosensors with Distinct Biomechanical Properties Allow for Specificity in Mechanotransduction

J. W. Frey,[†] E. E. Farley,[†] T. K. O'Neil,[†] T. J. Burkholder,[‡] and T. A. Hornberger[†*]
[†]Department of Comparative Biosciences, School of Veterinary Medicine, University of Wisconsin, Madison, Wisconsin 53706; and [‡]School of Applied Physiology, Georgia Institute of Technology, Atlanta, Georgia 30332

ABSTRACT Various cell types can sense and convert mechanical forces into biochemical signaling events through a process called mechanotransduction, and this process is often highly specific to the types of mechanical forces applied. However, the mechanism(s) that allow for specificity in mechanotransduction remain undefined. Thus, the goal of this study was to gain insight into how cells distinguish among specific types of mechanical information. To accomplish this goal, we determined if skeletal myoblasts can distinguish among differences in strain, strain rate, and strain-time integral (STI). Our results demonstrate that mechanically induced signaling through the c-jun N-terminal kinase 2 [JNK2] is elicited via a mechanism that depends on an interaction between the magnitude of strain and strain rate and is independent of STI. In contrast to JNK2, mechanically induced signaling through the ribosomal S6 kinase [p70(389)] is not strain rate sensitive, but instead involves a magnitude of strain and STI dependent mechanisms. Mathematical modeling also indicated that mechanically induced signaling through JNK2 and p70(389) can be isolated to separate viscous and elastic mechanosensory elements, respectively. Based on these results, we propose that skeletal myoblasts contain multiple mechanosensory elements with distinct biomechanical properties and that these distinct biomechanical properties provide a mechanism for specificity in mechanotransduction.

INTRODUCTION

A variety of cell types are sensitive to mechanical forces, including stem cells, cardiomyocytes, endothelial cells, smooth muscle cells, bone cells, and skeletal muscle cells (1–6). In these cell types, mechanical forces are converted into biochemical events through a process called mechanotransduction. The resulting biochemical events can regulate a variety of cellular and physiological processes, including changes in gene expression, cell size, proliferation, and morphogenesis, and the development of pathological diseases (7–14). Although the mechanosensing abilities of these various cell types have been recognized for decades, the basic properties of the mechanotransduction machinery remain largely undefined.

In recent years it has become apparent that cells not only sense mechanical information, but that the response to mechanical signals is often highly specific to the types of mechanical forces applied. For example, uniaxial and biaxial strains have been shown to induce distinct morphological, genetic, and biochemical signaling events in mesenchymal stem cells, skeletal myoblasts, and endothelial cells (6,15,16). Furthermore, distinct biochemical signaling events are activated when mechanical forces are applied axially and transversely to cardiac and skeletal muscle cells (17,18). Combined, these observations suggest that a variety of cell types are capable of sensing the direction through which mechanical forces are applied.

In addition to being able to sense the direction of mechanical forces, cells also appear to be able to sense the kinematic properties of mechanical forces. For example, dynamic mechanical strains promote an accumulation of bone mass, whereas an equivalent magnitude of static strain has no effect on bone mass (19). In skeletal muscle, mechanical loading with static stretch induces longitudinal hypertrophy (sarcomere deposition in-series with the long axes), whereas dynamic mechanical loading induces cross-sectional hypertrophy (sarcomere deposition in parallel with the long axes) (20). Furthermore, in skeletal muscle, isometric and lengthening contractions induce the expression of distinct genes, and this effect cannot be explained by differences in the magnitude of mechanical force applied to the tissue (21). Thus, various cell types appear to have the capacity to sense the kinematic properties of mechanical forces and the studies cited above (19–21) suggest that this may occur through distinct force- and velocity-dependent mechanosensors.

All of the aforementioned examples highlight the concept that mechanosensitive cells have the capacity to distinguish among specific types of mechanical information and therefore imply that specificity exists within the mechanosensing machinery. However, the concept of specificity within mechanotransduction is only beginning to be appreciated and the mechanisms that allow for this specificity remain to be defined. Thus, the goal of this study was to gain insight into how mechanosensitive cells, such as skeletal myoblasts, can distinguish among specific types of mechanical information.

To accomplish the goal of this study, we first tested the hypothesis that skeletal myoblasts can distinguish among differences in strain, strain rate, and the strain-time integral (STI). This was tested by subjecting C2C12 myoblasts

Submitted December 30, 2008, and accepted for publication April 14, 2009.

*Correspondence: thornb1@svm.vetmed.wisc.edu

Editor: Elliot L. Elson.

0006-3495/09/07/0347/10 $2.00

doi: 10.1016/j.bpj.2009.04.025

to biaxial strain, and the magnitude of strain, strain rate, and STI was systematically manipulated. Changes in the phosphorylation state of the c-jun N-terminal kinase 2 (JNK2) on the Thr^{183}/Tyr^{185} residues, as well as changes in the phosphorylation state of the ribosomal S6 kinase ($p70^{S6k}$) on the Thr^{389} residue, and the Thr^{421}/Ser^{424} residues, were used as markers of mechanotransduction. These molecules were selected for analysis because of their proposed roles in the transcriptional and translational regulation of various genes after mechanical stimulation (MS), respectively (22,23). Furthermore, several studies have shown that the phosphorylation state of these molecules is highly responsive to mechanical stimuli and thus, they can serve as excellent markers of mechanotransduction (24,25). In addition, the phosphorylation of JNK2, p70(389), and p70(421/424) have been shown to be regulated by distinct upstream signaling pathways (26–29). Therefore, a change in the phosphorylation state of these different sites would be expected to represent activation of signaling through distinct upstream pathways.

The results from this study demonstrate that mechanically induced signaling through JNK2 is elicited through a mechanism that is dependent on an interaction between the magnitude of strain and strain rate and independent of STI. In stark contrast to JNK2, mechanically induced signaling through $p70^{S6k}$ on the Thr^{389} residue [P-p70(389)] is not strain rate sensitive. Instead, mechanically induced signaling through p70(389) involves a mechanism that is dependent on the magnitude of strain and the STI. Combined, these results indicate that signaling through JNK2 and p70(389) is induced by distinct types of mechanical information. Furthermore, we developed a mathematical model to relate changes in JNK2 and p70(389) phosphorylation to the putative physical properties of the myoblasts. The results from this model indicate that signaling through JNK2 and p70(389) can be isolated to separate viscous and elastic mechanosensory elements, respectively. Thus, skeletal myoblasts appear to contain multiple mechanosensory elements with distinct biomechanical properties and these distinct biomechanical properties provide a mechanism for distinguishing among specific types of mechanical information. Taken together, this study provides evidence of a fundamental mechanism that allows for specificity in mechanotransduction.

MATERIALS AND METHODS

Materials

Rabbit primary antibodies, including anti-phospho-JNK2(Thr^{183}/Tyr^{185}), anti-phospho- $p70^{S6k}$(Thr^{421}/Ser^{424}), and anti-total $p70^{S6k}$ were purchased from Cell Signaling (Danvers, MA). Rabbit anti-phospsho-$p70^{S6k}$(Thr^{389}) was purchased from Santa Cruz Biotechnologies (Santa Cruz, CA). Anti-rabbit peroxidase-conjugated IgG (H+L) was purchased from Vector Laboratories (Burlingame, CA). Regular enhanced chemiluminescence (ECL) reagent was purchased from Pierce (Rockford, IL) and ECL plus reagent was purchased from Amersham (Piscataway, NJ).

Cell culture

Mouse C2C12 myoblasts were cultured in growth media consisting of high glucose DMEM (HyClone, Logan, UT) supplemented with antibiotics and antimycotics (penicillin G-100 U/mL, streptomycin-100 μg/mL and amphotericin-0.25 μg/mL) and 10% fetal bovine serum (Gibco, Grand Island, NY). For MS experiments, myoblasts were plated on Bioflex collagen I–coated 6-well dishes (Flexcell International, Hillsborough, NC) and grown to confluence. Upon confluence, the myoblasts were switched to antibiotic, antimycotic, and serum-free high-glucose DMEM for 18 h before being subjected to experimental treatments. This was done in an effort to minimize basal levels of p70(389) phosphorylation and maximize the observed mechanically induced changes in phosphorylation on this site. All cell culture experiments were performed in a humidified 95% air, 5% CO_2 incubator at 37°C.

MS

The Flexcell FX-4000T system (Flexcell International) was used to mechanically stimulate C2C12 myoblasts. This is a vacuum-operated system that produces biaxial (radial and circumferential) tensile strains (30). The MS programs employed on this device utilized triangular waveforms to produce 6%–18% biaxial strain at strain rates of 12%–36%/s and strain-time integrals of 1800%–5400%/s for 20 min. The specific waveforms used for each experiment are described in Figs. 1–3.

Western blot analysis

Immediately upon the completion of the MS protocol, the myoblasts were lysed in ice-cold buffer containing 40 mM Tris (pH 7.5), 1 mM EDTA, 5 mM EGTA, 0.5% Triton X-100, 25 mM β-glycerolphosphate, 25 mM NaF, 1 mM Na_3VO_4, 10 μg/mL leupeptin, and 1 mM PMSF. The lysate was centrifuged at 500 $\times$ g for 5 min and the supernatant was used for further analysis. The protein concentration of each sample was determined with the DC protein assay kit (Bio-Rad, Hercules, CA) and equivalent amounts of protein from each sample were subjected to Western blot analysis as previously described (31). Briefly, samples were dissolved in Laemmli buffer and subjected to electrophoretic separation by SDS-PAGE on 7.5% acrylamide gels. After electrophoretic separation, proteins were transferred to a PVDF membrane, blocked with 5% powdered milk in Tris-buffered saline, 1% Tween 20 (TBST) for 1 h, followed by an overnight incubation at 4°C with primary antibodies. After overnight incubation, the membranes were washed for 30 min in TBST and then probed with anti-rabbit peroxidase-conjugated secondary antibodies for 45 min at room temperature. After 30 min of washing in TBST, the blots were developed using regular ECL or ECL plus reagents. After capturing the appropriate images, the membranes were stained with Coomassie blue to verify equal loading in all lanes. Densitometric measurements were carried out using the public domain National Institutes of Health Image program (ImageJ) developed at the U.S. National Institutes of Health and available on the Internet at http://rsb.info.nih.gov/nih-image/.

Mathematical modeling

A three-element viscoelastic mechanical model was used to relate changes in JNK2 and p70(389) phosphorylation to the putative physical properties of the myoblasts (Fig. 4 *A*). This model has a single mathematical state, from which forces and deformations in each of the elements can be determined. The state equation for the model is:

$$\dot{x} = -\frac{k_1 + k_2}{b}x + \frac{k_2}{b}D,$$

where D is the applied deformation, x is the deformation of the parallel spring, k_1 is the stiffness of the parallel spring, k_2 is the stiffness of the series spring, and b is the viscosity of the viscous element.

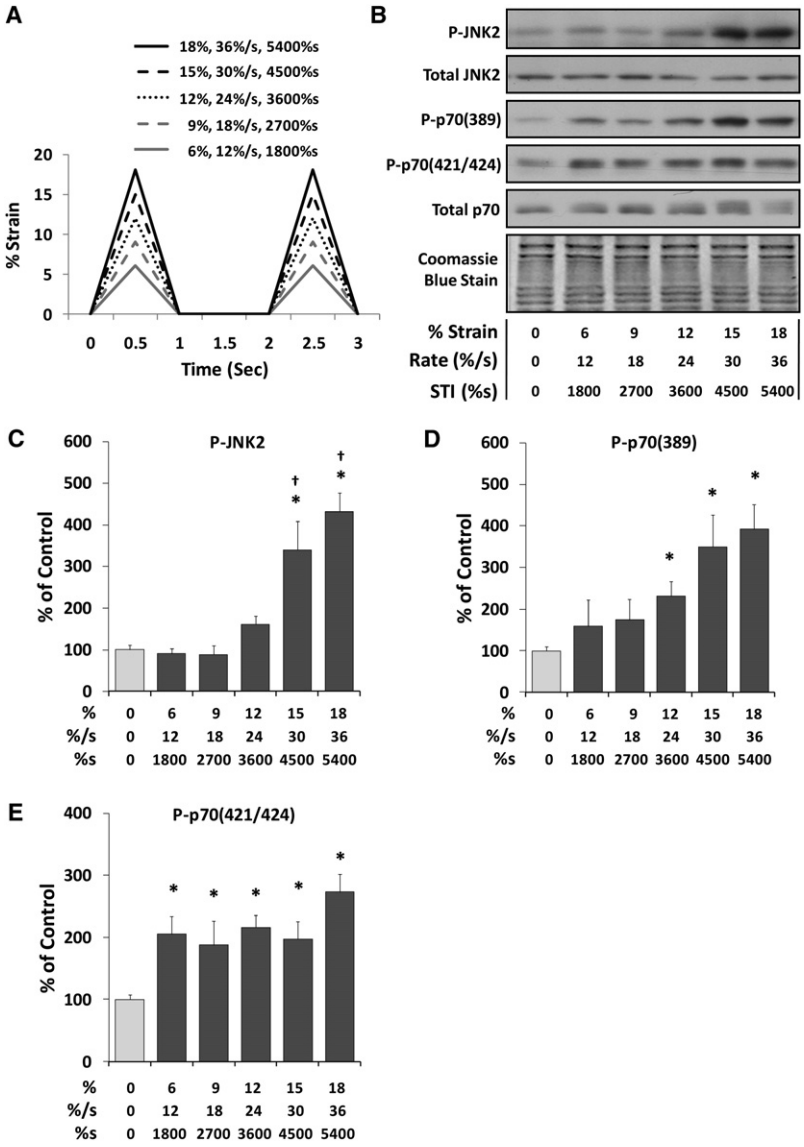

FIGURE 1 Activation of signaling through JNK2 and $p70^{S6k}$ in response to different magnitudes of mechanical stimulation. Confluent C2C12 myoblasts were grown on Bioflex collagen I–coated plates and serum starved for 18 h. (*A*) After the serum starvation, myoblasts were subjected to 20 min of cyclic mechanical stimulation with one of the waveforms described in *A* or held static as a control condition. Note: the different waveforms have progressively greater magnitudes of strain (%), strain rate (%/s), and strain-time integral (%s). After the bout of mechanical stimulation, samples were subjected to Western blot analysis for markers of signaling through JNK2 (P-JNK2) and $p70^{S6k}$ ([P-p70(389)] and [P-p70(421/424)]). Western blots of total JNK2 and total $p70^{S6k}$ protein, as well as Coomassie blue–stained Western blot membranes from 80–45 kDa, were used to verify equal loading of protein in all lanes. (*B*) Representative images of the Western blots and Coomassie blue–stained membranes (*C–E*). The images of P-JNK2 (*C*), P-p70(389) (*D*), and P-p70(421/424) (*E*) were quantified and the graphs represent the means ± SE expressed as a percentage of control ($n = 6$–17/group from ≥ 3 independent experiments). *Significantly different from control; †significantly different from the 9% strain, 18%/s strain rate, 2700 STI (%/s) group, ($p \leq 0.05$).

The steady-state solution of this equation for sinusoidal $D = \mathrm{A}\exp(j\,w\,t)$ is:

$$x = \frac{k_2}{k_1 + k_2 + jwb} D,$$

where t is time, w is frequency, and j is the square root of -1.

As described in the results, the mechanical activation of signaling through JNK2 was found to be dependent on an interaction between the magnitude of strain and the strain rate. This observation led us to hypothesize that mechanically induced changes in JNK2 phosphorylation would be proportional to force/stress in the viscous element b. Furthermore, changes in JNK2 phosphorylation were only detected when a critical combination of strain magnitude and strain rate was applied and this characteristic was modeled as a threshold stress response. On the other hand, changes in the phosphorylation of p70(389) were not dependent on strain rate, but instead showed a strong dependence on the magnitude of strain applied to the myoblasts. Based on this observation, we hypothesized that changes in p70(389) phosphorylation resulted from deformation of the k_2 spring. For sinusoidal D, the phosphorylation of these molecules was estimated as:

$$\frac{p70}{D} = C_1 \frac{k_1 + jwb}{k_1 + k_2 + jwb},$$

$$\frac{JNK}{D} = C_2 \left(\frac{k_2 w}{wb - j(k_1 + k_2)} - T \right),$$

where C_1 is the gain of p70(389) phosphorylation, C_2 is the gain of JNK phosphorylation, and T is a threshold strain rate.

Changes in both p70(389) and JNK2 phosphorylation in response to various mechanical perturbations were available from 180 different trials. These data points were transformed to zero mean and unit variance and used to estimate the model parameters (C_1, C_2, and T) by nonlinear least squares regression using the Nelder-Mead algorithm (MATLAB fminsearch, The MathWorks, Natick, MA).

Statistical analysis

All values are expressed as means ± SE. For Western blot analyses, statistical significance was determined by one-way or two-way ANOVA,

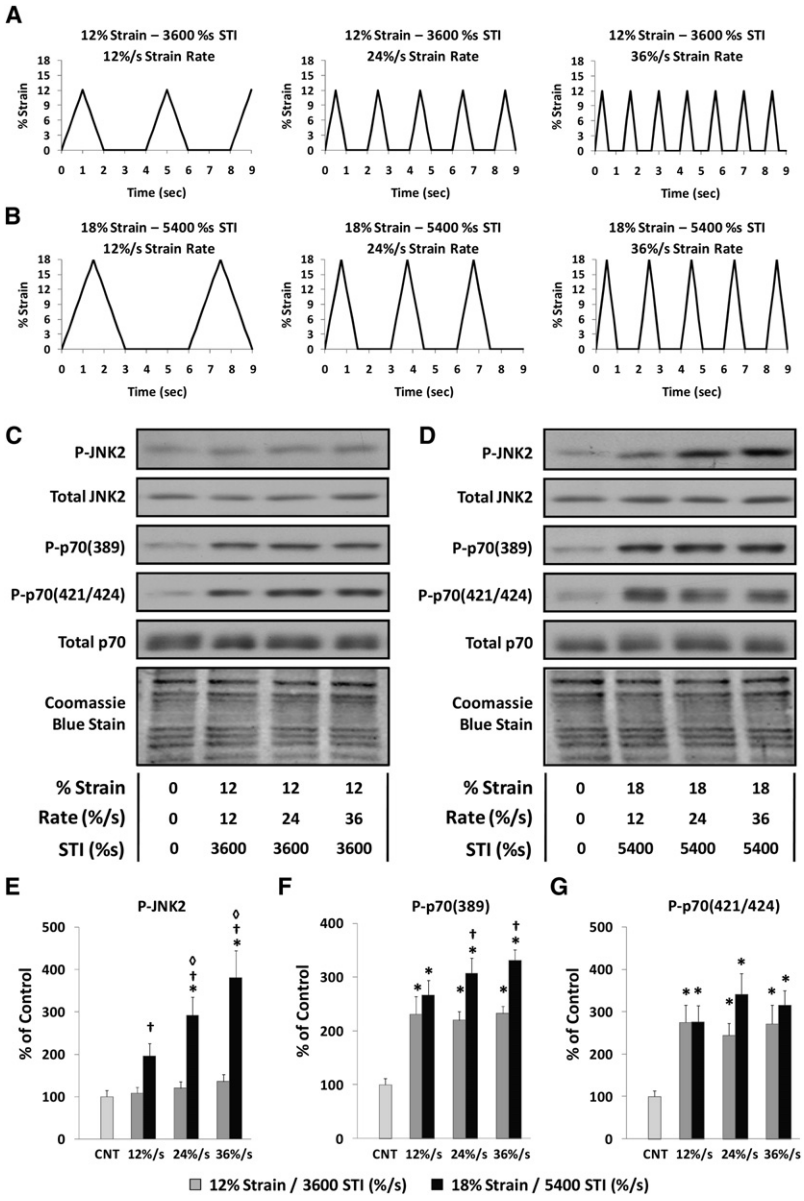

FIGURE 2 The role of strain rate in the mechanical activation of signaling through JNK2 and p70^{S6k}. Confluent C2C12 myoblasts were grown on Bioflex collagen I–coated plates and serum starved for 18 h. After the serum starvation, myoblasts were subjected to 20 min of cyclic 12% strain with a 3600%s STI using the strain rates indicated by the waveforms in *A*, or subjected to 20 min of cyclic 18% strain with a 5400%/s STI using the strain rates indicated by the waveforms in *B*. Serum-starved myoblasts were also held static for 20 min as a control condition. All samples were subjected to Western blot analysis for markers of signaling through JNK2 (P-JNK2) and p70^{S6k} ([P-p70(389)] and [P-p70(421/424)]). Western blots of total JNK2 and total p70^{S6k} protein, as well as Coomassie blue–stained Western blot membranes from 80–45 kDa, were used to verify equal loading of protein in all lanes. (*C*) Representative images of the Western blots and Coomassie blue–stained membranes subjected to the waveforms described in *A*. (*D*) Representative images of the Western blots and Coomassie blue–stained membranes from samples subjected to the waveforms described in *B*. (*E–G*) The images of P-JNK2 (*E*), P-p70(389) (*F*), and P-p70(421/424) (*G*) were quantified and the graphs represent the means ± SE expressed as a percentage of control ($n = 9$–16 / group from ≥ 3 independent experiments). *Significantly different from control; †significantly different from 12% strain/3600 STI (%/s) at the indicated strain rate; ◇significantly different from 12%/s strain rate within the 18% strain/5400 STI (%/s) groups, ($p \leq 0.05$).

followed by Student Newman-Keuls post hoc analysis. Differences between groups were considered significant if $p \leq 0.05$. Statistical analyses of the Western blot data were performed on SigmaStat software (San Jose, CA). Statistical analyses for the mathematical model were performed in MATLAB (Novi, MI).

RESULTS

Activation of signaling through JNK2 and p70^{S6k} in response to different magnitudes of mechanical stimulation

C2C12 myoblasts were subjected to 20 min of MS with various magnitudes of strain, strain rate, and STI using the waveforms described in Fig. 1 *A*. The activation of signaling through JNK2 was monitored by evaluating changes in Thr^{183}/Tyr^{185} phosphorylation [P-JNK2], and the activation of signaling through p70^{S6k} was evaluated by measuring changes in Thr^{389} phosphorylation [P-p70(389)] and Thr^{421}/Ser^{424} phosphorylation [P-p70(421/424)]. The results identified three distinct activation patterns that can be described as i), nonlinear (threshold) increase in signaling through JNK2 as the magnitude of MS increased (Fig. 1, *B* and *C*) ii), linear ($R^2 = 0.91$) increase in signaling through p70(389) as the magnitude of MS increased (Fig. 1, *B* and *D*), and iii), maximum activation of signaling through p70(421/424) at all of magnitudes of MS (Fig. 1, *B* and *E*). These observations suggested that the activation of signaling through JNK2, p70(389), and p70(421/424) is sensitive to different mechanical parameters and therefore may involve distinct mechanosensory elements.

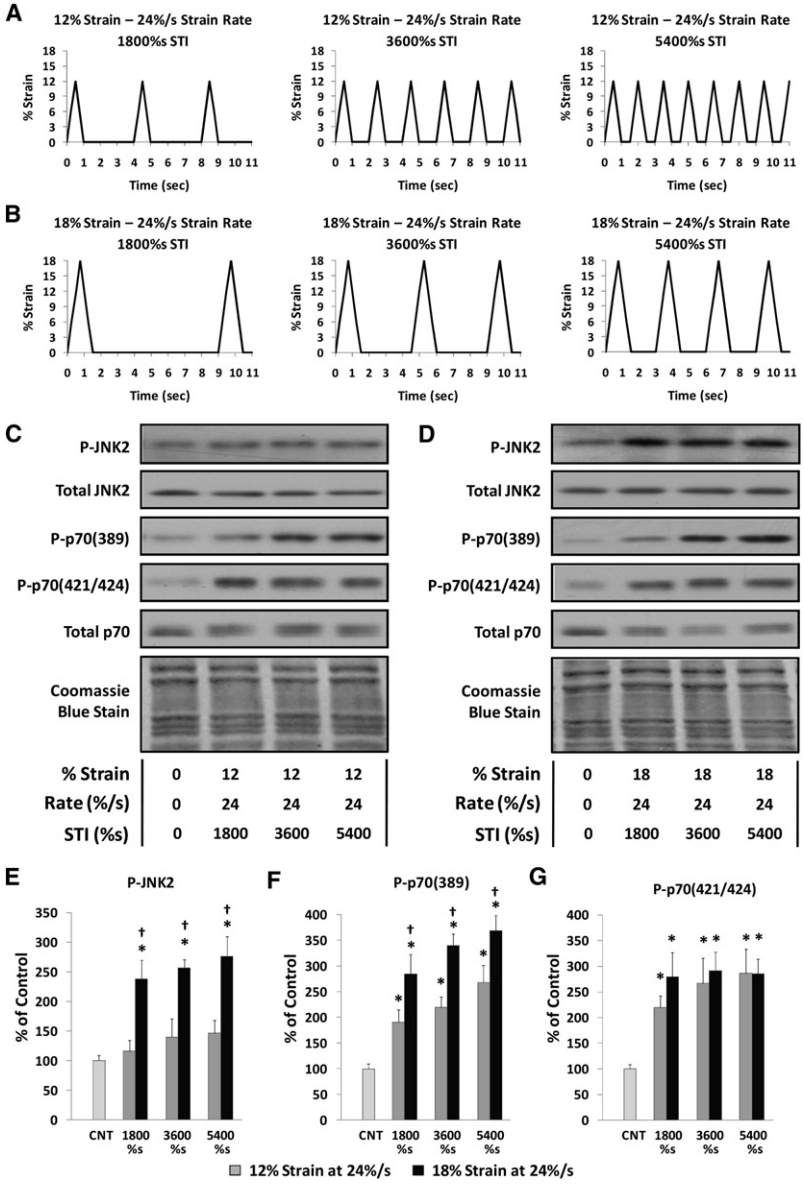

FIGURE 3 The role of strain and strain-time integral in the mechanical activation of signaling through JNK2 and $p70^{S6k}$. Confluent C2C12 myoblasts were grown on Bioflex collagen I–coated plates and serum starved for 18 h. After the serum starvation, myoblasts were subjected to 20 min of cyclic 12% strain with a 24%/s strain rate using the strain-time integrals (STI) indicated by the waveforms in *A*, or subjected to 20 min of cyclic 18% strain with a 24%/s strain rate using the STI indicated by the waveforms in *B*. Serum-starved myoblasts were also held static for 20 min as a control condition. All samples were subjected to Western blot analysis for markers of signaling through JNK2 (P-JNK2) and $p70^{S6k}$ ([P-p70(389)] and [P-p70(421/424)]). Western blots of total JNK2 and total $p70^{S6k}$ protein, as well as Coomassie blue–stained Western blot membranes from 80–45 kDa, were used to verify equal loading of protein in all lanes. (*C*) Representative images of the Western blots and Coomassie blue–stained membranes from samples subjected to the waveforms described in *A*. (*D*) Representative images of the Western blots and Coomassie blue–stained membranes from samples subjected to the waveforms described in *B*. (*E–G*) The images of P-JNK2 (*E*), P-p70(389) (*F*) and P-p70(421/424) (*G*) were quantified and the graphs represent the means ± SE expressed as a percentage of control ($n = 5$–17/group from ≥ 3 independent experiments). *Significantly different from control; †significantly different from 12% strain/24%/s strain rate at the indicated STI (%/s), ($p \leq 0.05$).

The role of strain rate in the mechanical activation of signaling through JNK2 and $p70^{S6k}$

To define the mechanical parameters that were responsible for the activation of signaling through JNK2, p70(389) and p70(421/424), we first investigated the role of strain rate. To accomplish this, C2C12 myoblasts were subjected to 20 min of MS at different strain rates while holding the magnitude of strain and STI constant. In these experiments, the magnitude of strain was held at 12% and the STI was held at 3600%/s using the waveforms described in Fig. 2 *A*, or held at 18% strain and 5400%/s STI using the waveforms described in Fig. 2 *B*.

The results from these experiments indicated that signaling through JNK2 was not significantly activated at any of strain rates employed in the 12% strain/3600%/s STI conditions (Fig. 2, *C* and *E*). However, in the 18% strain/5400%/s STI conditions, signaling through JNK2 was activated at all of the strain rates employed, and the magnitude of activation was highly dependent on the strain rate (Fig. 2, *D* and *E*). Further statistical analysis of these results also revealed that the activation of signaling through JNK2 was due to an interaction between the magnitude of strain/STI and the magnitude of the strain rate (Table 1).

Unlike JNK2, signaling through p70(389) was activated at all of the strain rates employed and this occurred in both the 12% strain/3600%/s STI and 18% strain/5400%/s STI conditions (Fig. 2, *C*, *D*, and *F*). Although p70(389) phosphorylation appeared to show a weak strain rate dependence at 18% strain, these differences did not reach statistical significance and there was no support for an interaction between strain and strain rate ($p = 0.35$). However, the activation of

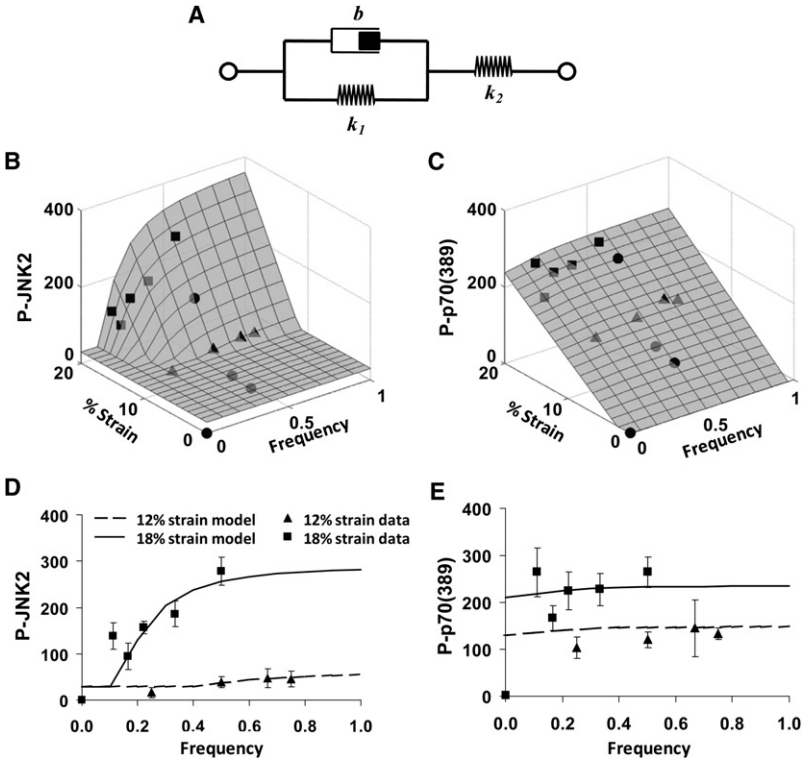

FIGURE 4 Viscoelastic model of mechanically induced signaling through JNK2 and p70^{S6k}. Nonlinear regression in combination with a three-element viscoelastic mechanical model *A* was used to predict changes in JNK2 and p70(389) phosphorylation as a function of strain magnitude and strain rate/frequency (see Methods for details). (*B–C*) The predicted increase in JNK2 phosphorylation *B* and p70(389) phosphorylation *C* as a function of strain magnitude and strain rate/frequency is shown as three-dimensional surface plots. For comparative purposes, the average values from 180 trails of data obtained in myoblasts subjected to different combinations of strain magnitude and strain rate/frequency are shown as single points (▲,■,●) within the three-dimensional grid. Points falling above the surface are shown in black and points falling below the surface are shown in gray. (*D–E*) Slices through the predicted three-dimensional surfaces at 12% strain (*dashed lines*) and 18% strain (*solid lines*) are presented in combination with the data obtained for JNK2 phosphorylation (*D*) and p70^{S6k}(389) phosphorylation (*E*) in myoblasts subjected to 12% strain (▲) and 18% strain (■) at various strain rates/frequencies.

signaling through p70(389) was sensitive to the magnitude of strain/STI (Fig. 2 *F* and Table 1). Taken together, these results indicate that the mechanical activation of signaling through p70(389) is sensitive to the magnitude of strain and/or STI, but not strain rate.

Similar to p70(389), signaling through p70(421/424) was activated at all of the strain rates employed and this occurred when the myoblasts were subjected to either the 12% strain/3600%/s STI or the 18% strain/5400%/s STI conditions (Fig. 2, *C*, *D*, and *G*). However, neither the magnitude of the strain rate or the magnitude of the strain/STI had a significant effect on the activation of signaling through p70(421/424) (Fig. 2 *G* and Table 1). These results indicate that the mechanical activation of signaling through p70(421/424) was not sensitive to the magnitudes of strain, STI, or strain rate employed in this study. However, signaling through p70(421/424) appeared to be at a maximum in all of the strains, STIs, and strain rates employed. Thus, it remains possible that the activation of signaling through p70(421/424) is sensitive to these mechanical parameters, and if this sensitivity does exist, it likely occurs at much lower magnitudes than those employed in this study.

TABLE 1 Summary of the statistical main effects and interactions that were observed for the data presented in Fig. 2.

	Main effect of strain rate	vs.	Main effect of strain/STI	Significant interaction
P-JNK2	+		+	+
P-p70(389)	−		+	−
P-p70(421/424)	−		−	−

+ Significant main effect or interaction.
$p \leq 0.05$.

Combined, the results from this series of experiments demonstrate that the mechanical activation of signaling through JNK2, p70(389) and p70(421/424) is regulated by different types of mechanical information and therefore suggest that signaling through these molecules may be induced through distinct mechanosensory elements.

The role of strain and strain-time integral in the mechanical activation of signaling through JNK2 and p70^{S6k}

The results from the experiments described above indicate that the mechanical activation of signaling through both JNK2 and p70(389) is sensitive to the magnitude of strain and/or STI. To define the role of strain and STI in these responses, myoblasts were subjected to 20 min of MS at various magnitudes of STI while holding the magnitude of strain and the strain rate constant. In these experiments, the magnitude of strain was held at 12% and the strain rate at 24%/s using the waveforms described in Fig. 3 *A*, or at 18% strain and 24%/s strain rate using the waveforms described in Fig. 3 *B*.

The results from these experiments indicated that signaling through JNK2 was not activated at any of STIs employed in the 12% strain/24%/s strain rate conditions (Fig. 3, *C* and *E*). However, in the 18% strain/24%/s strain rate conditions, signaling through JNK2 was activated at all of the

STIs employed. Furthermore, the amount of signaling through JNK2 was not dependent on the magnitude of the STI (Fig. 3, *D*, and *E* and Table 2). These results demonstrate that the magnitude of strain, but not STI, plays a critical role in the mechanical activation of signaling through JNK2. When combined with the results from Fig. 2, these experiments indicate that the mechanical stimuli activate signaling through JNK2 via a mechanosensory element that is responsive to an interaction between the magnitude of strain and strain rate and is independent of STI.

In contrast to JNK2, signaling through p70(389) was activated at all of the STIs employed, and this occurred in both the 12% strain/24%/s strain rate and 18% strain/24%/s strain rate conditions. In addition, the amount of signaling through p70(389) was found to be dependent on the magnitude of STI in both the 12% strain/24%/s strain rate and 18% strain/24%/s strain rate conditions (Fig. 3, *C*, *D*, and *F*). Furthermore, at each STI, signaling through p70(389) was greater in the 18% strain/24%/s strain rate condition. Taken together, these results demonstrate that both the magnitude of strain and the magnitude of the STI play a key role in the activation of signaling through p70(389) (Table 2). When combined with the results from Fig. 2, these experiments indicate that mechanical stimuli activate signaling through p70(389) via a mechanosensory element that is responsive to the magnitude of strain and the magnitude of STI, but not strain rate.

Similar to p70(389), signaling through p70(421/424) was activated at all of the STIs employed and this occurred when the myoblasts were subjected to either the 12% strain/24%/s strain rate or the 18% strain/24%/s strain rate conditions (Fig. 3, *C*, *D*, and *G*). However, neither the magnitude of the strain or STI significantly altered the amount of signaling through p70(421/424) (Fig. 3 *G* and Table 2). Thus, consistent with the results from Fig. 2, mechanically induced signaling through p70(421/424) appeared to be the maximum in all of the conditions, and therefore did not reveal a sensitivity to the magnitudes of strain and STI that were employed.

Viscoelastic model of mechanically induced signaling through JNK2 and p70^{S6k}

Nonlinear regression was used to predict changes in JNK2 and p70(389) phosphorylation as a function of strain magnitude and strain rate (frequency) using the three-element viscoelastic mechanical model described in the Methods section (Fig. 4 *A*). The predicted increase in JNK2 and p70(389) phosphorylation from this model as a function of strain magnitude and strain rate (frequency) is shown as three-dimensional surface plots in Fig. 4 *B* and Fig. 4 *C*, respectively. For comparative purposes, the average values from data obtained in myoblasts subjected to different combinations of strain magnitude and strain rate (frequency), as reported in Figs. 1–3, are shown as single data points within the three-dimensional grids. Points falling above the surface are shown in black and points falling below the surface are shown in gray. These graphs demonstrate that the model was able to accurately predict the mechanically induced increase in JNK2 and p70(389) phosphorylation. To further illustrate this point, slices through the predicted three-dimensional surfaces were compared with the data obtained for JNK2 phosphorylation (Fig. 4 *D*) and p70(389) phosphorylation (Fig. 4 *E*) in myoblasts subjected to 12% strain and 18% strain at various strain rates (frequencies). Again, these graphs reveal that the model yielded accurate predictions of the mechanically induced increase in JNK2 and p70(389) phosphorylation. One of the most striking features of this model is that it also accurately predicted the unique threshold relationship between strain, strain rate, and signaling through JNK2. According to the model, it is nearly impossible to induce JNK2 phosphorylation at strain magnitudes lower than 11%, and this prediction is highly consistent with the results obtained in this study.

The mathematical model produced a coefficient of determination (R^2) of 0.41 and $f_{(7,170)}$ of 9.83, yielding a $p < 10^{-9}$. For comparison, multiple linear regression to this data produce R^2 of 0.36 and $f_{(3,175)}$ of 49. Only relative mechanical parameters could be derived from the model and it was determined that k_1, k_2, and b had values of 9.3, 1.0, and 61.7, respectively. Thus, the k_1 spring was ~9 times more compliant than the viscoelastic element, and the system had a time constant $(b/k_1 + k_2)$ of 5.7 s. The threshold, T, was 0.18/s and essentially identical to the reciprocal of the time constant.

TABLE 2 Summary of the statistical main effects and interactions that were observed for the data presented in Fig. 3.

	Main effect of strain	vs.	Main effect of STI	Significant interaction
P-JNK2	+		−	−
P-p70(389)	+		+	−
P-p70(421/424)	−		−	−

+ Significant main effect or interaction.
$p \leq 0.05$.

DISCUSSION

The mechanosensing abilities of various cells types have been recognized for decades. More recently it has become apparent that cells can not only sense mechanical information, but the response to mechanical signals is often very specific to the types of mechanical forces applied. The resulting biochemical events that are elicited by specific types of mechanical information ultimately regulate distinct processes, including changes in gene expression, cell size, proliferation, and morphogenesis, and development of pathological disease (7–14). This point is particularly important when one considers that a wide range of diseases within virtually all fields of medicine result from abnormal mechanotransduction (12,14). Thus, developing a comprehensive understanding of

how cells sense and respond to mechanical information could have a broad impact on a variety of areas in biomedical research.

Although numerous studies indicate that cells have the capacity to distinguish among specific types of mechanical information, the mechanisms that allow for this specificity remain largely undefined. In this study, we provide evidence that skeletal myoblasts contain multiple mechanosensory elements that have distinct biomechanical properties and these distinct biomechanical properties could provide a mechanism for myoblasts to distinguish among specific types of mechanical information. In particular, the results support the hypothesis that mechanical stimuli activate signaling through JNK2 after a threshold of stress is generated within a mechanosensory element that contains viscous properties. On the other hand, mechanical stimuli appear to activate signaling through p70(389) via a mechanosensory element that contains linear, spring-like properties. Furthermore, as shown in Fig. S1 in the Supporting Material, disrupting the actin cytoskeleton with cytochalasin D blocks the mechanical activation of signaling through both JNK2 and p70(389). Thus, although the mechanical activation of signaling through JNK2 and p70(389) appears to be regulated by two distinct mechanosensory elements, both of these mechanosensory elements require an intact actin cytoskeleton for activation.

Based on the results from this study, we have developed a conceptual model of an actin cytoskeleton dependent mechanosensor that could elicit both viscous and linear, spring-like behaviors (Fig. 5). In this conceptual model, the ends of the mechanosensor are linked to the actin cytoskeleton and force transmission through the actin cytoskeleton is necessary for inducing deformations of the mechanosensor. Within the mechanosensor, there are two independent sensory elements coupled in series. One of the sensory elements promotes signaling through JNK2 [P-JNK2 responder] and the other promotes signaling through p70(389) [P-p70(389) responder]. In both cases, signaling is stimulated when the responder binds to cryptic activation sites. Under resting conditions, the cryptic activation sites are inaccessible and no signaling occurs (Fig. 5 *A*). However, when the appropriate mechanical information is applied, the cryptic activation sites reach an open state and initiate a cascade of signaling events that ultimately result in JNK2 and/or p70(389) phosphorylation (Fig. 5 *B*).

In this conceptual model (Fig. 5), we have selected the lipid membrane to represent the viscous mechanosensory

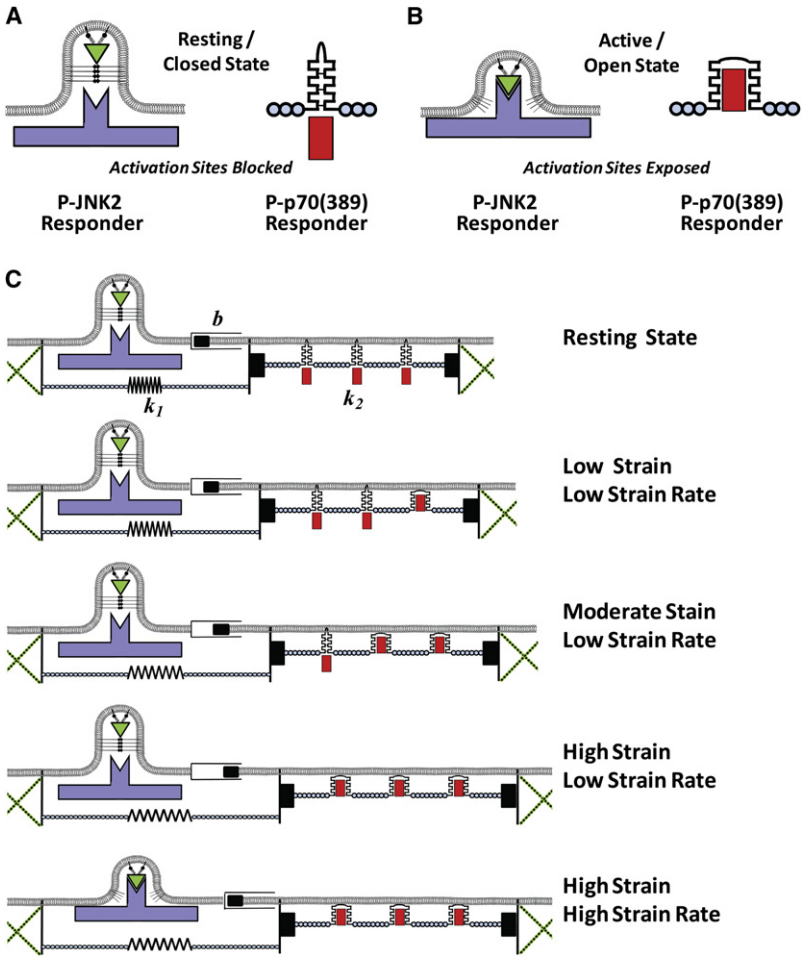

FIGURE 5 Conceptual model of a mechanosensor that induces signaling through JNK2 and $p70^{S6k}$. The mechanosensor contains two independent sensory elements and requires an intact actin cytoskeleton (••••) for mechanical deformations to occur. One of the sensory elements promotes signaling through JNK2 [P-JNK2 responder] and the other promotes signaling through p70(389) [P-p70(389) responder]. In both cases, signaling is stimulated when the responder binds to cryptic activation sites. (*A*) Under resting conditions the cryptic activation sites are in a closed state and no signaling occurs. (*B*) When the appropriate mechanical information is applied, the cryptic activation sites reach an open state, and in turn, initiate a cascade of signaling events which ultimately result in JNK2 and/or p70(389) phosphorylation. (*C*) A detailed explanation of how specific types of mechanical information expose the cryptic activation sites for the P-JNK2 and P-p70(389) responder are provided in the Discussion section.

element (b) that responds to the types of mechanical information that activate signaling through JNK2. In the resting state, the cryptic activation site for the P-JNK2 responder is positioned in a closed state. In response to slow deformations (low strain rate), the membrane can flow/remodel and the resulting stress is borne by the elastic elements k_1 and k_2. As a result, the stress-dependent cryptic activation site for the JNK2 responder remains in the closed state. However, in response to faster deformations (high strain rate), the membrane is not able to flow/remodel and stress accumulates in the membrane. If the resulting stress exceeds the threshold (T), the cryptic activation site for the JNK2 responder reaches an open state and induces a cascade of signaling events that ultimately result in JNK2 phosphorylation (Fig. 5 *C*).

On the other hand, a protein with linear, spring-like properties represents the mechanosensory element (k_2) that responds to the types of mechanical information that activate signaling through p70(389). In this mechanosensory element, there are multiple cryptic activation sites for the p70(389) responder and the probability of these sites reaching the active/open state is directly related to the magnitude of strain. At low magnitudes of strain, only a small proportion of the cryptic activation sites reach the open state and, as a result, only a small induction of signaling through the pathway that leads to p70(389) phosphorylation would occur. As the magnitude of strain increases, the number of cryptic activation sites reaching the open state progressively increases and, as a result, a progressively greater amount of signaling through the pathway that leads to p70(389) phosphorylation is achieved. It should also be noted that the data from this study indicate that both the magnitude of strain and the STI play a role in the activation of signaling through p70(389). Consistent with this data, it could be argued that the probability of the p70(389) responder binding to the cryptic activation site is dependent on how long the activation site remains in the open state. Thus, at higher STIs there is a greater probability that the p70(389) responder will bind to the activation site and induce subsequent downstream signaling. Under this argument, the mechanosensor would yield both strain and STI dependent signaling through p70(389) (Fig. 5 *C*).

With the exception of the actin cytoskeleton, this study does not identify a particular molecule or structural element as being critical in mechanotransduction. Instead, this study highlights the fact that a wide variety of molecules/structures have been implicated in mechanotransduction, including stretch-activated ion channels, caveolae, integrins, cadherins, growth factor receptors, myosin motors, various cytoskeletal proteins, nuclei, the extracellular matrix, and numerous other structures (1,32–35). The long list of molecules/structures implicated in mechanotransduction is consistent with the hypothesis that cells contain multiple mechanosensory elements. Based on the results of this study, we propose that many of these mechanosensory elements do not function independently, but instead require mechanical integration with structural elements such as the actin cytoskeleton. Furthermore, we propose that many of the mechanosensory elements in cells have distinct biomechanical properties, and that having multiple mechanosensory elements with distinct biomechanical properties provides a mechanism for cells to respond to specific types of mechanical information.

SUPPORTING MATERIAL

One figure is available at http://www.biophysj.org/biophysj/supplemental/S0006-3495(09)00855-8.

This work was supported by a National Institutes of Health grant AR053280 to T.A.H.

REFERENCES

1. Linke, W. A. 2008. Sense and stretchability: the role of titin and titin-associated proteins in myocardial stress-sensing and mechanical dysfunction. *Cardiovasc. Res.* 77:637–648.
2. Chien, S. 2007. Mechanotransduction and endothelial cell homeostasis: the wisdom of the cell. *Am. J. Physiol. Heart Circ. Physiol.* 292:H1209–H1224.
3. Haga, J. H., Y. S. Li, and S. Chien. 2007. Molecular basis of the effects of mechanical stretch on vascular smooth muscle cells. *J. Biomech.* 40:947–960.
4. Robling, A. G., A. B. Castillo, and C. H. Turner. 2006. Biomechanical and molecular regulation of bone remodeling. *Annu. Rev. Biomed. Eng.* 8:455–498.
5. Hornberger, T. A., and K. A. Esser. 2004. Mechanotransduction and the regulation of protein synthesis in skeletal muscle. *Proc. Nutr. Soc.* 63:331–335.
6. Park, J. S., J. S. Chu, C. Cheng, F. Chen, D. Chen, et al. 2004. Differential effects of equiaxial and uniaxial strain on mesenchymal stem cells. *Biotechnol. Bioeng.* 88:359–368.
7. Jaalouk, D. E., and J. Lammerding. 2009. Mechanotransduction gone awry. *Nat. Rev. Mol. Cell Biol.* 10:63–73.
8. Ingber, D. E., L. Dike, L. Hansen, S. Karp, H. Liley, et al. 1994. Cellular tensegrity: exploring how mechanical changes in the cytoskeleton regulate cell growth, migration, and tissue pattern during morphogenesis. *Int. Rev. Cytol.* 150:173–224.
9. Henderson, J. H., and D. R. Carter. 2002. Mechanical induction in limb morphogenesis: the role of growth-generated strains and pressures. *Bone.* 31:645–653.
10. Ko, K. S., and C. A. McCulloch. 2001. Intercellular mechanotransduction: cellular circuits that coordinate tissue responses to mechanical loading. *Biochem. Biophys. Res. Commun.* 285:1077–1083.
11. Goldspink, G., A. Scutt, P. T. Loughna, D. J. Wells, T. Jaenicke, et al. 1992. Gene expression in skeletal muscle in response to stretch and force generation. *Am. J. Physiol.* 262:R356–R363.
12. Ingber, D. E. 2003. Mechanobiology and diseases of mechanotransduction. *Ann. Med.* 35:564–577.
13. Wozniak, M. A., and C. S. Chen. 2009. Mechanotransduction in development: a growing role for contractility. *Nat. Rev. Mol. Cell Biol.* 10:34–43.
14. Wang, N., J. D. Tytell, and D. E. Ingber. 2009. Mechanotransduction at a distance: mechanically coupling the extracellular matrix with the nucleus. *Nat. Rev. Mol. Cell Biol.* 10:75–82.
15. Hornberger, T. A., D. D. Armstrong, T. J. Koh, T. J. Burkholder, and K. A. Esser. 2005. Intracellular signaling specificity in response to uniaxial vs. multiaxial stretch: implications for mechanotransduction. *Am. J. Physiol. Cell Physiol.* 288:C185–C194.
16. Wang, J. H., P. Goldschmidt-Clermont, J. Wille, and F. C. Yin. 2001. Specificity of endothelial cell reorientation in response to cyclic mechanical stretching. *J. Biomech.* 34:1563–1572.

17. Kumar, A., I. Chaudhry, M. B. Reid, and A. M. Boriek. 2002. Distinct signaling pathways are activated in response to mechanical stress applied axially and transversely to skeletal muscle fibers. *J. Biol. Chem.* 277:46493–46503.

18. Gopalan, S. M., C. Flaim, S. N. Bhatia, M. Hoshijima, R. Knoell, et al. 2003. Anisotropic stretch-induced hypertrophy in neonatal ventricular myocytes micropatterned on deformable elastomers. *Biotechnol. Bioeng.* 81:578–587.

19. Lanyon, L. E., and C. T. Rubin. 1984. Static vs dynamic loads as an influence on bone remodelling. *J. Biomech.* 17:897–905.

20. Russell, B., D. Motlagh, and W. W. Ashley. 2000. Form follows function: how muscle shape is regulated by work. *J. Appl. Physiol.* 88:1127–1132.

21. Hentzen, E. R., M. Lahey, D. Peters, L. Mathew, I. A. Barash, et al. 2006. Stress-dependent and -independent expression of the myogenic regulatory factors and the MARP genes after eccentric contractions in rats. *J. Physiol.* 570:157–167.

22. Boppart, M. D., M. F. Hirshman, K. Sakamoto, R. A. Fielding, and L. J. Goodyear. 2001. Static stretch increases c-Jun NH2-terminal kinase activity and p38 phosphorylation in rat skeletal muscle. *Am. J. Physiol. Cell Physiol.* 280:C352–C358.

23. Baar, K., and K. Esser. 1999. Phosphorylation of p70(S6k) correlates with increased skeletal muscle mass following resistance exercise. *Am. J. Physiol.* 276:C120–C127.

24. Martineau, L. C., and P. F. Gardiner. 2001. Insight into skeletal muscle mechanotransduction: MAPK activation is quantitatively related to tension. *J. Appl. Physiol.* 91:693–702.

25. Baar, K., G. Nader, and S. Bodine. 2006. Resistance exercise, muscle loading/unloading and the control of muscle mass. *Essays Biochem.* 42:61–74.

26. Hornberger, T. A., R. Stuppard, K. E. Conley, M. J. Fedele, M. L. Fiorotto, et al. 2004. Mechanical stimuli regulate rapamycin-sensitive signalling by a phosphoinositide 3-kinase-, protein kinase B- and growth factor-independent mechanism. *Biochem. J.* 380:795–804.

27. Hornberger, T. A., W. K. Chu, Y. W. Mak, J. W. Hsiung, S. A. Huang, et al. 2006. The role of phospholipase D and phosphatidic acid in the mechanical activation of mTOR signaling in skeletal muscle. *Proc. Natl. Acad. Sci. USA.* 103:4741–4746.

28. Wang, X., A. Destrument, and C. Tournier. 2007. Physiological roles of MKK4 and MKK7: insights from animal models. *Biochim. Biophys. Acta.* 1773:1349–1357.

29. Dufner, A., and G. Thomas. 1999. Ribosomal S6 kinase signaling and the control of translation. *Exp. Cell Res.* 253:100–109.

30. Gilbert, J. A., P. S. Weinhold, A. J. Banes, G. W. Link, and G. L. Jones. 1994. Strain profiles for circular cell culture plates containing flexible surfaces employed to mechanically deform cells in vitro. *J. Biomech.* 27:1169–1177.

31. Hornberger, T. A., K. B. Sukhija, X. R. Wang, and S. Chien. 2007. mTOR is the rapamycin-sensitive kinase that confers mechanically-induced phosphorylation of the hydrophobic motif site Thr(389) in p70(S6k). *FEBS Lett.* 581:4562–4566.

32. Ingber, D. E. 2006. Cellular mechanotransduction: putting all the pieces together again. *FASEB J.* 20:811–827.

33. Burkholder, T. J. 2007. Mechanotransduction in skeletal muscle. *Front. Biosci.* 12:174–191.

34. Schwartz, M. A., and D. W. DeSimone. 2008. Cell adhesion receptors in mechanotransduction. *Curr. Opin. Cell Biol.* 20:551–556.

35. Gieni, R. S., and M. J. Hendzel. 2008. Mechanotransduction from the ECM to the genome: are the pieces now in place? *J. Cell. Biochem.* 104:1964–1987.